Science Advances
AAAS

Supplementary Materials for

An ultrathin rechargeable solid-state zinc ion fiber battery for electronic textiles

Xiao Xiao, Xiao Xiao, Yihao Zhou, Xun Zhao, Guorui Chen, Zixiao Liu, Zihan Wang, Chengyue Lu, Menglei Hu, Ardo Nashalian, Sophia Shen, Kedi Xie, Weiwei Yang, Yongji Gong*, Wenbo Ding, Peyman Servati, Chao Han, Shi Xue Dou, Weijie Li*, Jun Chen*

*Corresponding author. Email: yongjigong@buaa.edu.cn (Y.G.); wl347@uowmail.edu.au (W.L.); jun.chen@ucla.edu (J.C.)

Published 1 December 2021 *Sci. Adv.* **7**, eabl3742 (2021)
DOI: 10.1126/sciadv.abl3742

The PDF file includes:

Other Supplementary Material for this manuscript includes the following:

Supplementary Text

1. Characterizations of GPHE and ZIB fiber

1.1. Fabrication costs and energy density of ZIB fiber The as-prepared zinc ion battery fiber is an all-in-one solid cylinder-like object. Therefore, we can directly weigh it and record the mass on the electronic balance, marked as: 0.4526 g, 0.4513 g, 0.4576 g, 0.4532 g and 0.4436 g. The average mass of the ZIB fiber batteries is 0.4516 g and standard deviation is 0.00237. The effective value is marked as 0.45 g. The diameter of the battery is determined by the diameter of 3D-printed photosensitive resin mould, which is accurately machined into 1 mm. The cost of a single battery fiber is calculated plainly as the sum of each proportion listed in the equation:

$$W_{all} = W_{cathode} + W_{anode} + W_{electrolyte} + W_{coating}$$

Every single wire of 15 cm fiber battery requires 18 cm zinc wire (0.3mm diameter) and 18 cm carbon wire (1K diameter), and GPHE solution of approximately 0.471 cm^3 (a 15-centimeter-tall-cylinder with 1 mm diameter). For cathode, the cost of carbon wire (SOVETL fiber) is 0.92 $ per meter, while the cost of slurry coating for each wire can be gently calculated by:

$$W_{slurry} = 0.05 \times (2.87 \times 10^{-3}\ \mathrm{kg} \cdot 2474.28\ \$ \cdot \mathrm{kg}^{-1} + 0.755 \times 10^{-3}\ \mathrm{kg} \cdot 242.78\ \$ \cdot \mathrm{kg}^{-1})$$

The unit price of each ingredient is listed corresponding to Supplementary table 2, while the ratio 0.05 is an empirical constant represents that each group of cathode materials prepared by hydrothermal method is capable of coating on about 20 wire cathodes, considering the loss. On the other hand, the cost of zinc wire (Daoguan) is 0.31 $ per meter, so that the cost of anode can be calculated similarly. The cost of electrolytes and coating are calculated as below, corresponding to Supplementary table 2.

$$W_{electrolyte} = \frac{0.471}{50} \times (4.25 \times 10^{-3}\ \mathrm{kg} \cdot 230.41\ \$ \cdot \mathrm{kg}^{-1} + 1420 \times 10^{-3}\ \mathrm{L} \cdot 1.53\ \$ \cdot \mathrm{L}^{-1})$$

$$W_{coating} = \frac{1}{20} \times 0.03\mathrm{kg} \cdot 16.87\ \$ \cdot \mathrm{kg}^{-1}$$

As a result, the overall cost of a single ZIB battery fiber is:

$$W_{all} = 0.92 \times 0.18 + 0.31 \times 0.18 + 0.3642 + 0.0297 + 0.0253 = 0.64\ \$$$

1.2. Volume energy density calculation of ZIB fiber According to the primitive data file of Fig. 4H, the discharge capacity of a 15 cm ZIB fiber is 10.71 mWh, calculated by an integration of the closed area of CV curve. Meanwhile, we have the volume $V = (0.05\ \mathrm{cm})^2 \times \pi \times 15\ \mathrm{cm} = 0.12\ \mathrm{cm}^3$. So, the volume energy density is achieved as follows:

$$E_v = \frac{10.71\ \text{mWh}}{0.12\ \text{cm}^3} = 91\ \text{mWh} \cdot \text{cm}^{-3}$$

2. Characterizations of GPHE and ZIB fiber

2.1. Stress-strain curve and modulus The mechanical properties of GPHEs of different GO mass components were measured by a tensile testing device (Cellscale Univert mechanical tester). The GPHEs were solidified in dog-bone-shaped 3D-printed resin moulds with a width of 2 mm and thickness 1 mm. The stress-strain curves were obtained by dividing the measured force by the cross-section area and dividing the measured displacement by the clamp distance. Fifteen hydrogel specimens were tested for each GO fraction (0, 0.16, 0.32, 0.48, 0.64 wt.%) and salt solution concentrations (0.5 M, 1.0 M, and 2.0 M).

2.2. Spectra characterizations: Raman, XRD and SAXS Raman analysis was carried out on a bench Raman dispersive micro spectrometer (InVia Reflex, Renishaw) using a laser (wavelength of 532 nm) at frequencies from 500 to 3500 cm^{-1}. Infrared-vis spectrum characterization was carried out on an infrared spectrometer (Nicolet IS10) with a range from 285 to 2000 nm. XRD and Small Angle X-ray Scattering (SAXS) measurements were carried out on a Bruker D8-Advance powder X-ray diffractometer operating at 40 kV and 30 mA, using Cu-Kα radiation (λ = 0.15405 nm). Thermal analysis was carried out on a Thermogravimetric analyzer (NETZSCH STA 449 F5/F3 Jupiter) with heating range from RT to 650 ℃, 10 ℃/min.

2.3. Scanning electron microscopy SEM images were obtained by a SU8020 Field emission SEM instrument. nano-MnO_2 cathodes were gently washed with deionized water to remove the electrolyte and dried for 12 h in a vacuum at 85 °C prior to the characterizations. Electrolytes (GPHEs) were gently washed with deionized water to remove salt solutions and freeze-drying for 2 days in advance.

2.4. Inductive coupled plasma When the soaking process comes to an end, a balance of Zn^{2+} and Mn^{2+} concentration inside the polymer gel and salt solution was achieved. Then, 5 uL of the salt solution was taken after the soaking process and diluted to 50 ppm to prepare the sample for ICP testing (Agilent ICPMS7800).

2.5. Electrochemical impedance spectroscopy The ionic conductivity of GPHEs was measured by electrochemical impedance spectroscopy (EIS) measurements with AC potential amplitude of 10 mV and frequency range of 1 Hz-100 kHz. The A.C. Impedance results were fitted in software Zviewer for a Nyquist plot under the equivalent circuit of the LC oscillation circuit. At high frequency (100 kHz), the corresponding value of the intercept on the real axis (x-axis) represents the intrinsic resistance of ion gel as the ohmic resistance of the testing devices is negligible. The ion conductivity is calculated according to:

$$\sigma = \frac{L}{R \times S}$$

where σ is the ionic conductivity, L is the distance between two electrodes, R is the impedance resistance of ion gels, and S is the geometric area of the electrode/electrolyte interface. The ionic mobility was calculated according to:

$$u_{(x_1 x_2 \ldots\ldots x_i)} = \frac{\sum_{i=0}^{n} t(x_i)}{\sum_{i=0}^{n} c(x_i)}$$

where u is the ionic mobility ratio of each ion component, t is the ionic mobility number and c is the overall concentration of each ion component. Meanwhile, ionic migration number t was calculated according to:

$$t_{(x_1 x_2 \ldots\ldots x_i)} = \frac{\sigma}{\sum_{i=0}^{n} \nu_i \cdot \lambda_{mi}}$$

Where σ is the ionic conductivity of the as-prepared gel electrolyte, ν represents the ratio of ion component to total concentration, and λ_{m} is the limiting molar conductance of each component measured in nearly infinite dilution solution.

2.6. Battery test The as-prepared GPHEs were fabricated as conventional stacked type, all-in-one type coin cells and aqueous cells by the steps mentioned above. To figure out the specific redox reactions during the charge and discharge process, we conducted cyclic voltammetry testing of each type of coin cell at a scan rate of 0.05 $mV \cdot s^{-1}$ (Fig. 3B). The rate performance characterization was tested under the set rates of 0.2 C, 0.5 C, 2.0 C, 5.0 C, 20 C, and 50 C (Fig. 3D). The coin cells were tested with a battery test system (NEWARE CT-4000) with a current density of 0.3 $A \cdot g^{-1}$ (Fig. 3E).

To demonstrate the effect of GPHEs optimization in prolonging the working life of flexible zinc ion batteries, we conducted long-term cycling for the conventional stacked type and all-in-one type zinc ion batteries with GPHE and PVA electrolytes, taking the aqueous electrolyte battery as a reference. The tests were performed under ambient conditions without replenishing the solution or replacing the zinc anode. The galvanostatic voltage profiles were collected at an absolute current density of 2 $mA \cdot g^{-1}$ with a time span of 30 min for each charging and discharging step (Fig. 3C).

2.7. Real-time scenario wearing test The performance of TBAN in reality were examined by a real-time mountain climbing scene. The wearable network system consisted of a microcontroller, a battery status monitor, a pulse sensor, a temperature/humid/atmospheric pressure sensor, all of which were integrated into the close-fitting cloth. Photographs and videos about TBAN exhibition, wireless reverse charging from the smartphone, and senor monitoring were recorded when one of the co-authors was wearing the cloth. Scenarios of testing varied from home environment to outdoor forest park.

Supplementary Figures

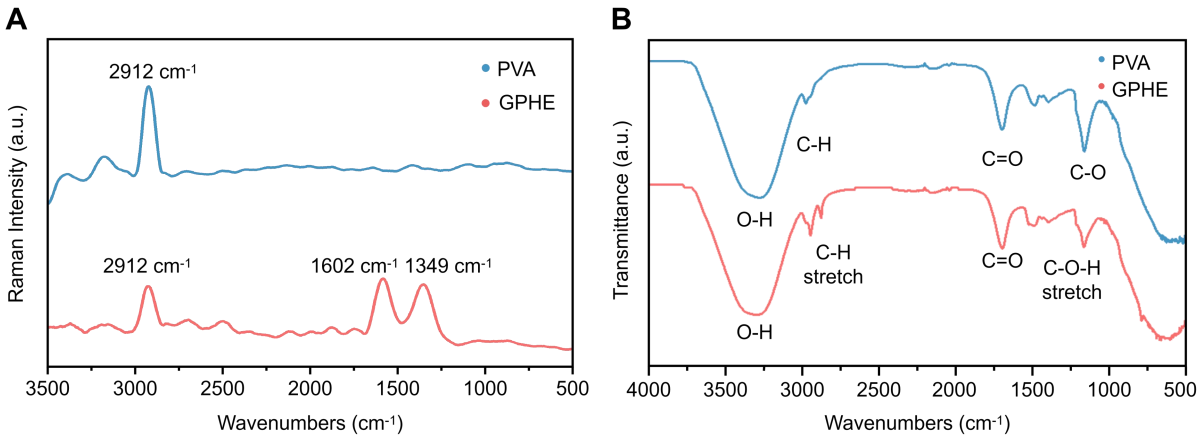

Figure S1. Spectral characterizations of bonding conditions in GPHE. (A) Raman spectra of GPHE, indicating clear D band (1349 cm^{-1}) and G band (1602 cm^{-1}) of GO to provide solid evidence for bonding between PVA polymer matrix and GO. (B) FTIR spectra, showing C-O bond and C-H bond stretch of PVA polymer molecular in GPHE. The stretch of C-H bond and O-H bond reveal the existence of different hydrogen bonds, which provide evidence for DFT calculation.

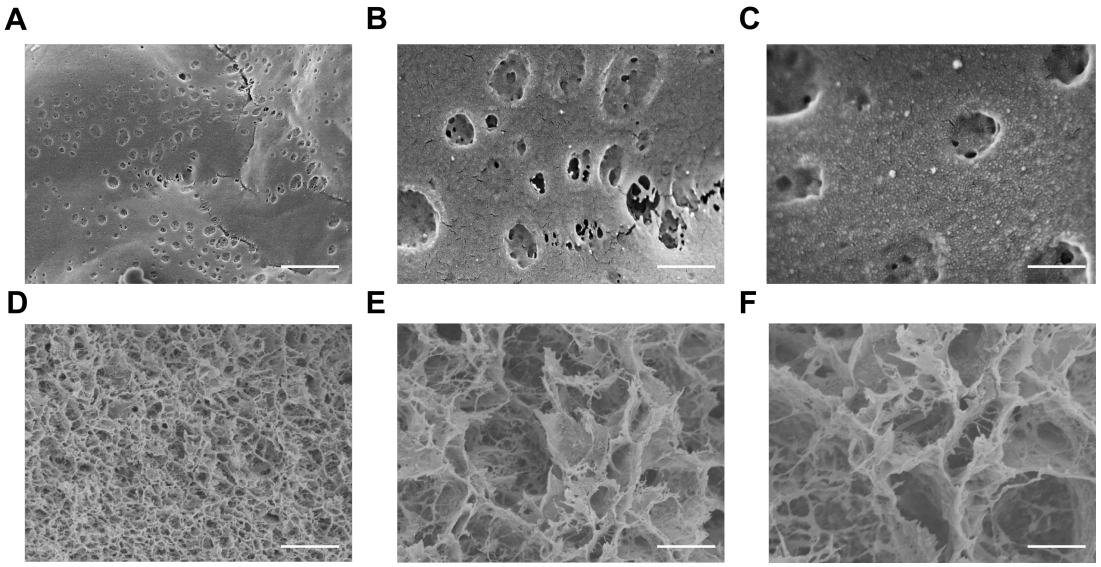

Figure S2. Scanning electron microscope (SEM) images of the channel-like micro-structures on GPHEs, which provide evidence for the establishment of "ion highway" model. Images of front view include (A) Scale bar, 5 μm, (B) Scale bar, 1 μm and (C) Scale bar, 500 nm and cross section view include (D) Scale bar, 50 μm, (E) Scale bar, 10 μm and (F) Scale bar, 5 μm.

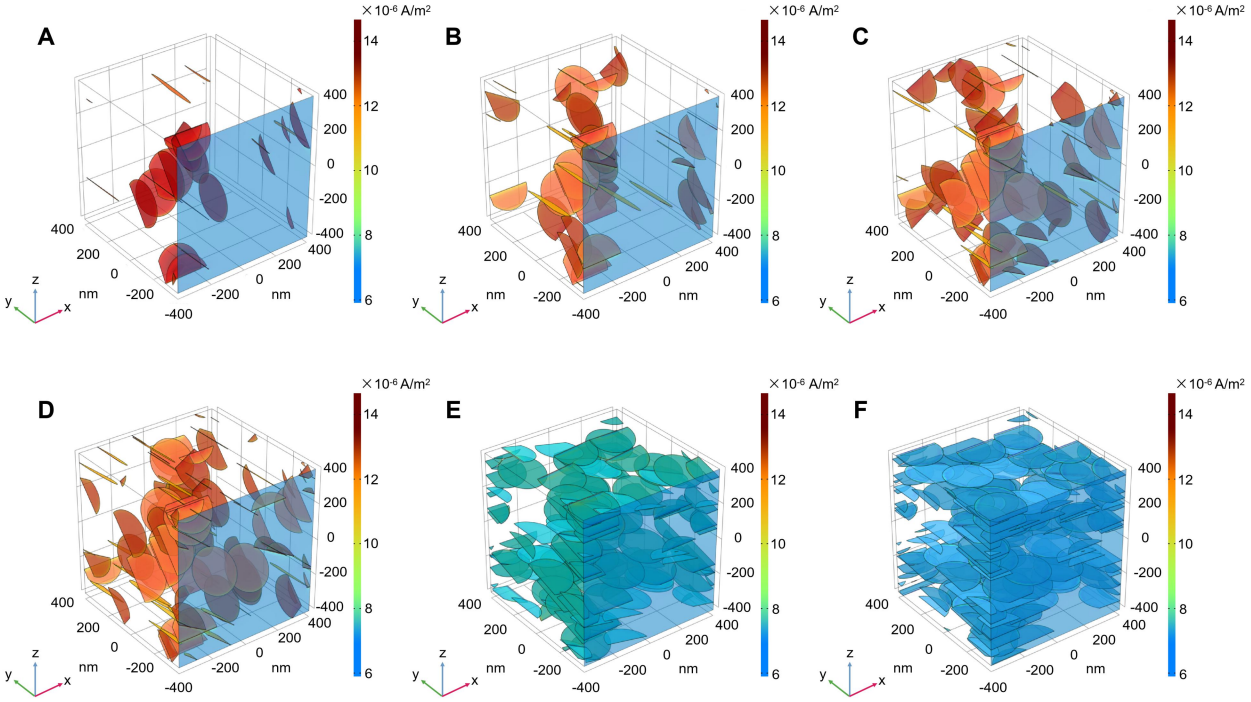

Figure S3. Finite element simulation of GPHE under different GO/PVA components: (A) 0.08 wt%. (B) 0.16 wt%. (C) 0.24 wt%. (D) 0.32 wt%. (E) 0.48 wt% and (F) 0.64 wt%.

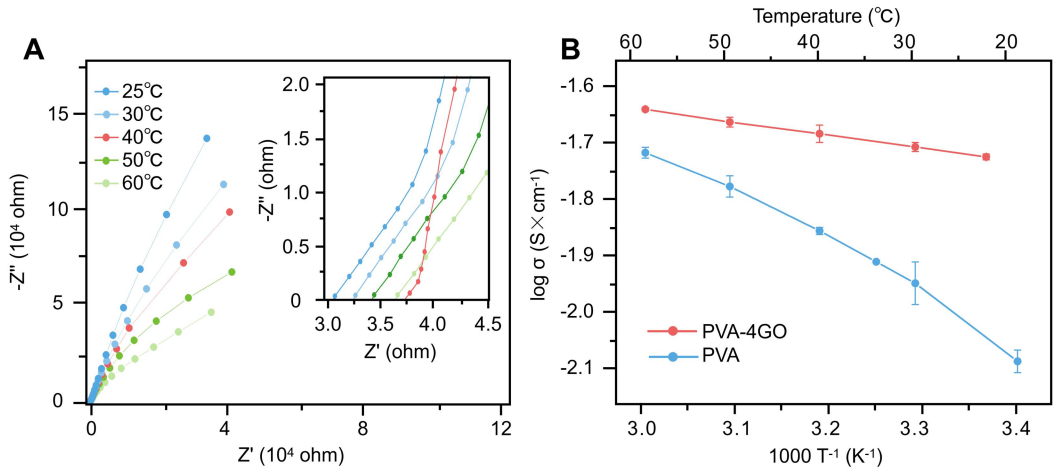

Figure S4. Thermal properties of PVA gel electrolyte and GPHE. (A) Ascending conductivity of GPHE under raising temperature. (B) Arrhenius plot comparison of GPHE and PVA electrolyte. The activation energy (***Ea***) is calculated from the Arrhenius equation. The lower ***Ea*** indicates that the GPHE could promote the Zn^{2+} transporting in polymer chains better than the PVA electrolyte with increased temperature. Error bar: error bars are standard deviations of GPHE samples under 25 ℃, 30 ℃, 40 ℃, 50 ℃, and 60 ℃.

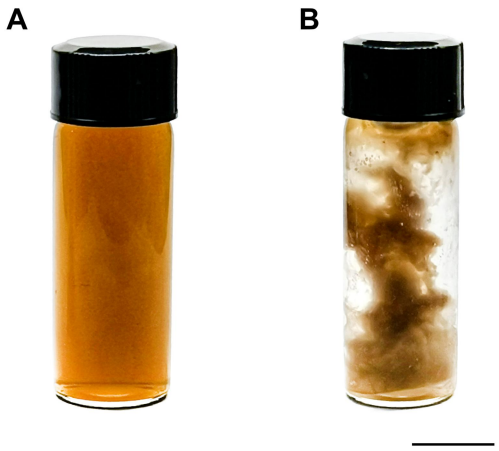

Figure S5. Precipitation effect of aqueous GPHE in salt solution. Photograph of gel aggregation by simple adding method: (A) before and (B) after. Scale bar, 2 cm. Photo Credit: Xiao Xiao, Beihang University.

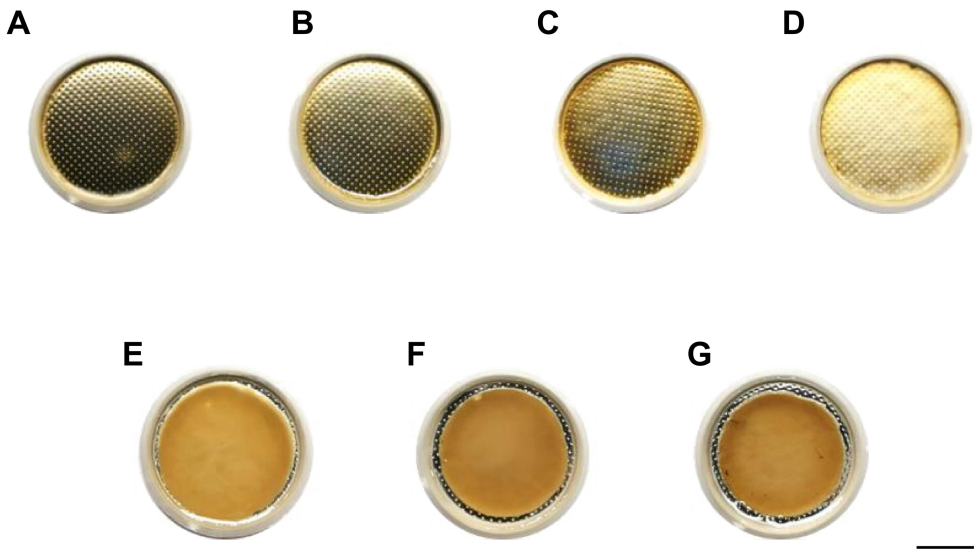

Figure S6. Photograph of preparation process of GPHE. (A) in liquid state, (B) after one cycle, (C) after two cycles and (D) after three cycles of freeze-thawing treatment. (E-G) the optimal images of GPHE absorbed in mixed $ZnSO_4$ and $MnSO_4$ salt solutions of: (E) 0.5 M $ZnSO_4$ + 0.3 M $MnSO_4$, (F) 1.0 M $ZnSO_4$ + 0.3 M $MnSO_4$ and (G) 2.0 M $ZnSO_4$ + 0.3 M $MnSO_4$. Scale bar, 1 cm. Photo Credit: Xiao Xiao, Beihang University.

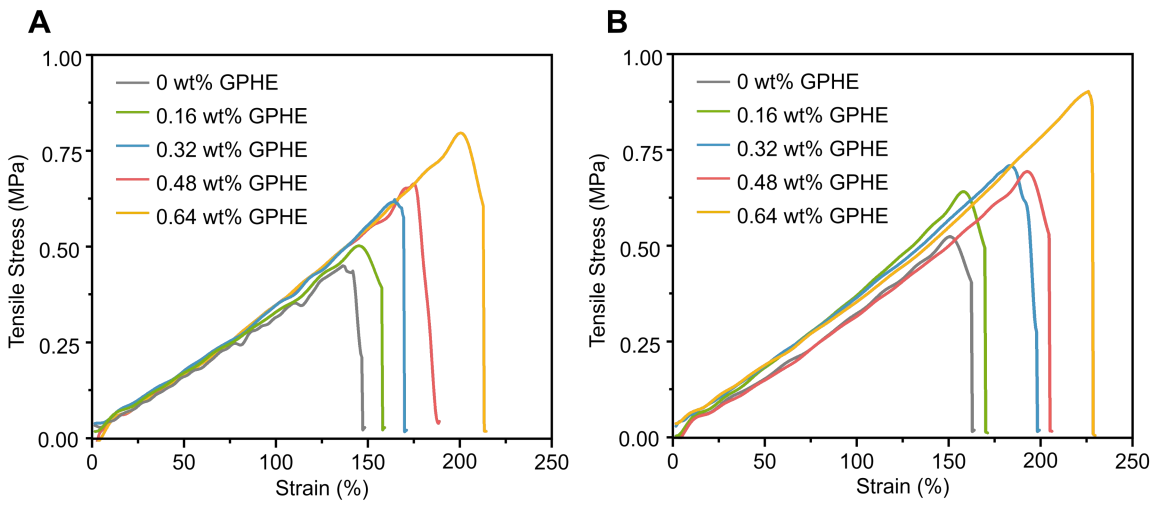

Figure S7. Tensile stress versus strain plots of the GPHE with different GO concentrations under (A) 0.5 M $ZnSO_4$/0.3M $MnSO_4$ and (B) 2.0M $ZnSO_4$/0.3M $MnSO_4$ as soaking salt solution. The rise of GO concentration results in the rise of tensile strength.

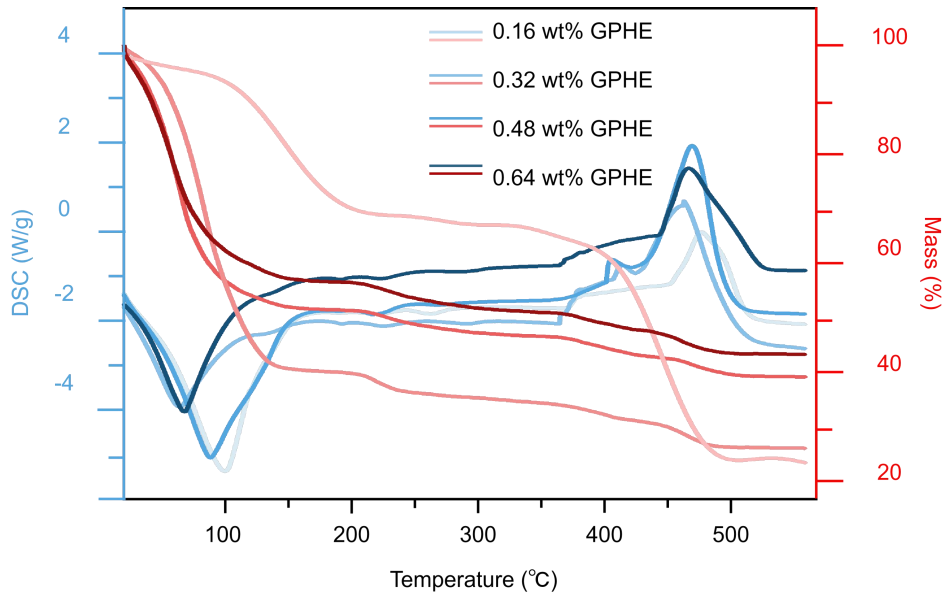

Figure S8. Differential scanning calorimetry (DSC) curves of GPHEs with different GO concentrations, indicating that when the mass fraction of GO increases, the hydrogen bonding sites for the H_2O molecular in the polymer decreases, thus the amount of wandering stage water grow up. Compared to the original PVA, larger amount of wandering stage water forms larger mass loss around 100 ℃.

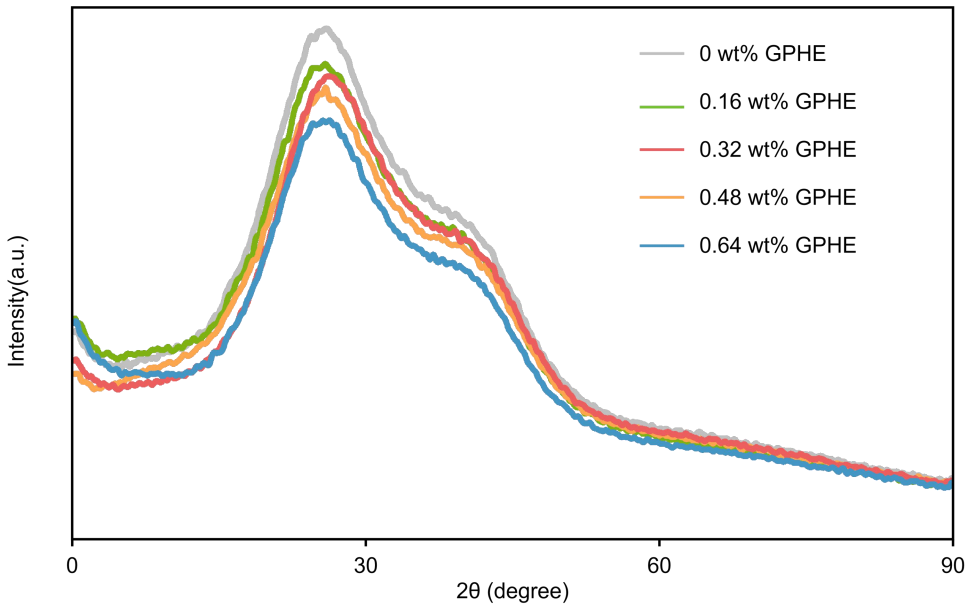

Figure S9. XRD curves of GPHE in different GO concentrations. As the mass fraction of GO increase, the crystallization peak of PVA decreases as a result of the hydrogen bonding between the PVA molecular and GO, which reduces the hydrogen bonding sites of H_2O molecular and forms more amorphous wandering water in the GPHE.

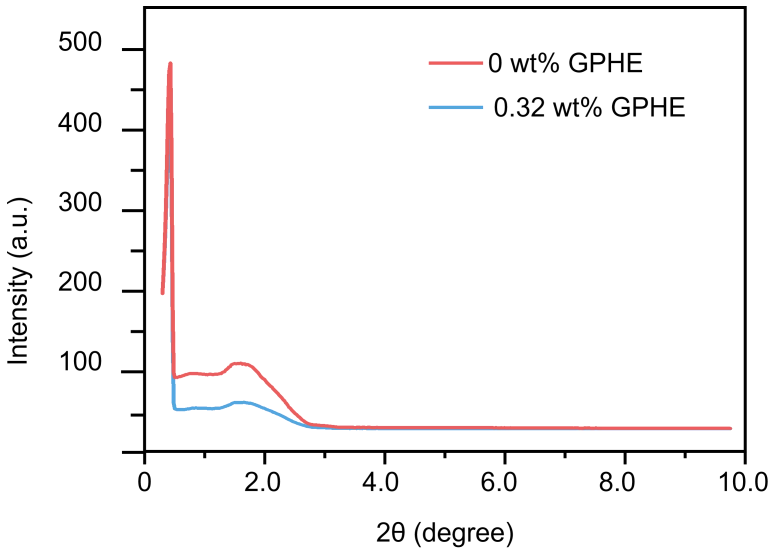

Figure S10. Small Angle X-ray Scattering (SAXS) curves of PVA electrolyte and 0.32 wt% GPHE showing a peak height change in 1°. The decrease of the peak at 2°provide evidence for the descending of crystalline degree after the adding of GO into the GPHE.

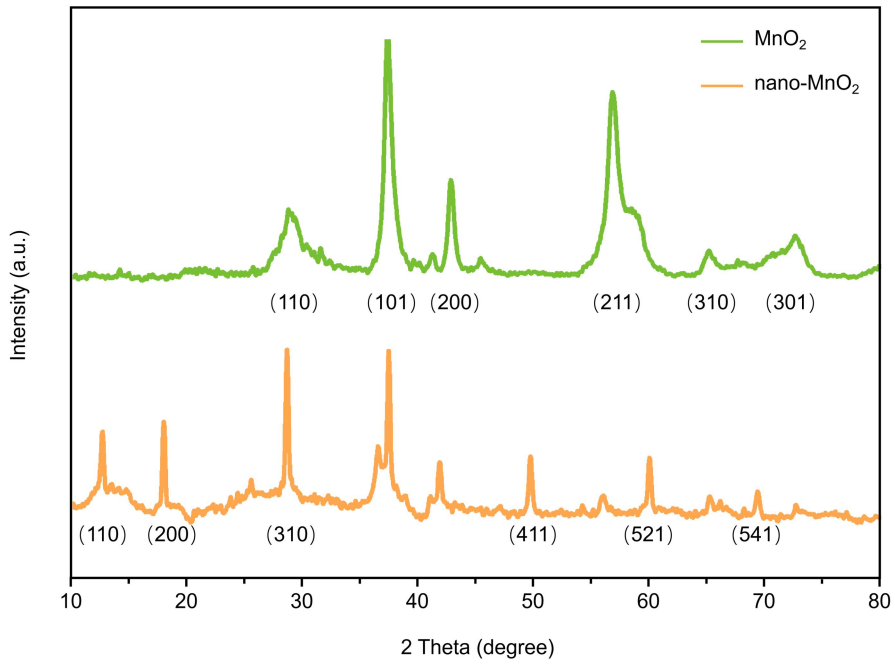

Figure S11. XRD curves of nano-MnO_2 and commercial MnO_2, revealing a higher crystallinity and more obvious two-dimensional structure.

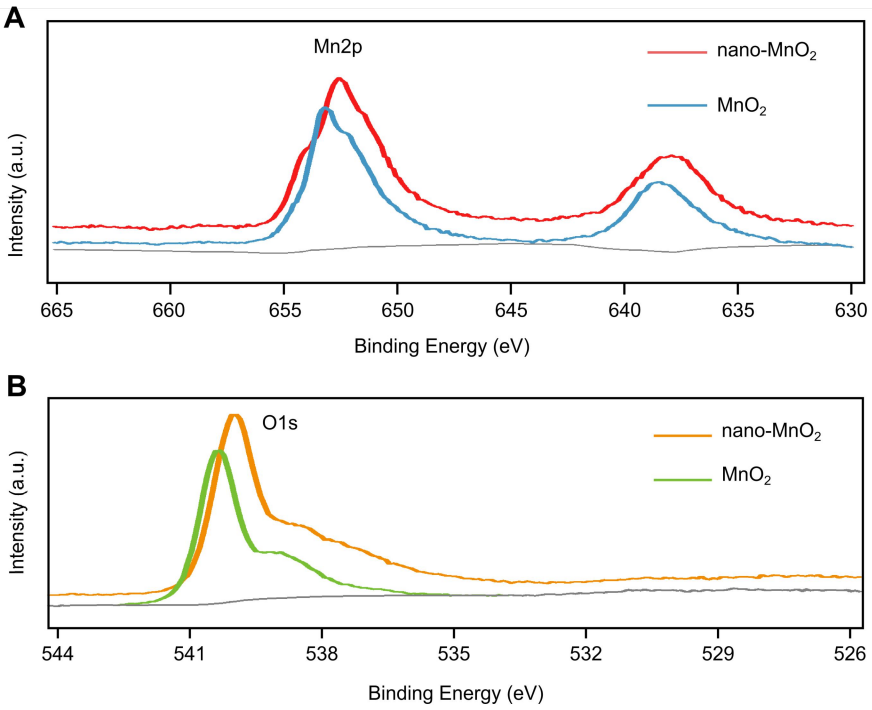

Figure S12. XPS curves of nano-MnO_2 and commercial MnO_2 revealing similar ways of bonding and hybridization by (A) Chemical shifting of Mn_{2p} doublet pairs and (B) O_{1s} peak.

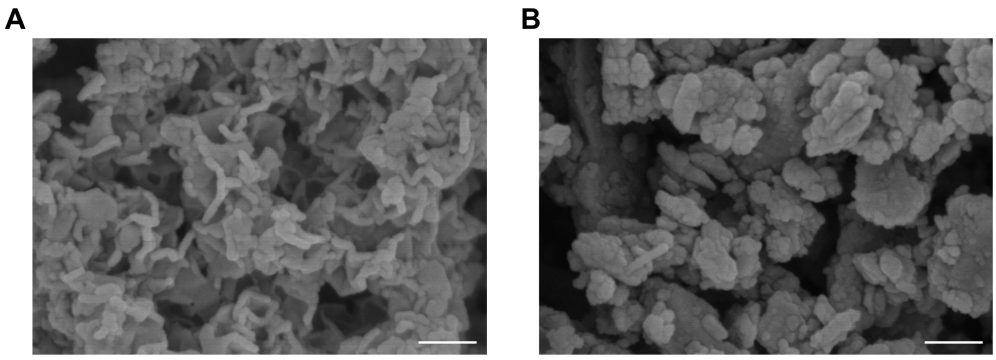

Figure S13. SEM images of (A) nano-MnO_2 and (B) commercial MnO_2 where a better way of bonding and hybridization is revealed in nano-MnO_2. Scale bars, 500 nm.

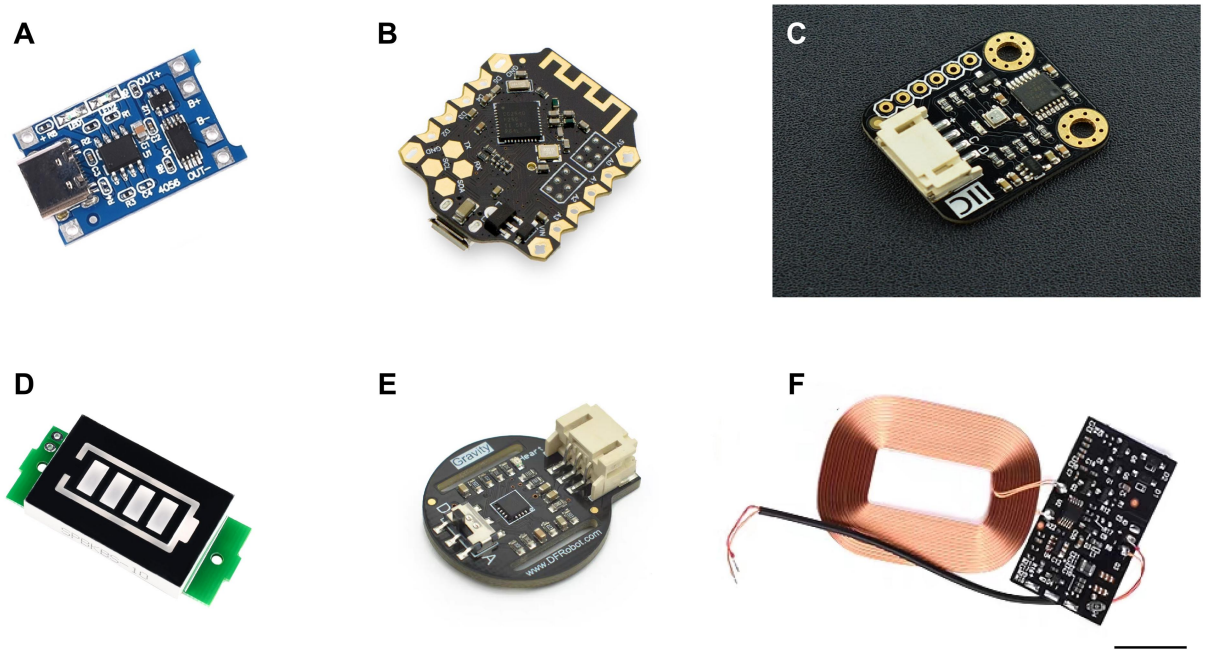

Figure S14. Wearable electronics on wireless textile body area network: (A) Protector. (B) Microcontroller. (C) Temperature/humid/atmospheric pressure sensor. (D) battery status monitor. (D) pulse sensor. (F) antenna for wireless charging. All scale bars, 1 cm. Photo Credit: DFRobot.

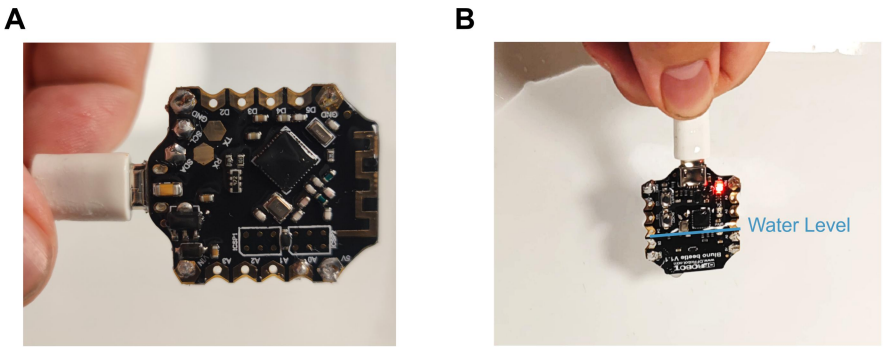

Figure S15. Water-proof PDMS coating on electronic components and sensors (represented by MCU): (A) MCU with water-proof coating. (B) Powered MCU absorbing in water, the power supply maintains stability. Photo Credit: Xiao Xiao, Beihang University.

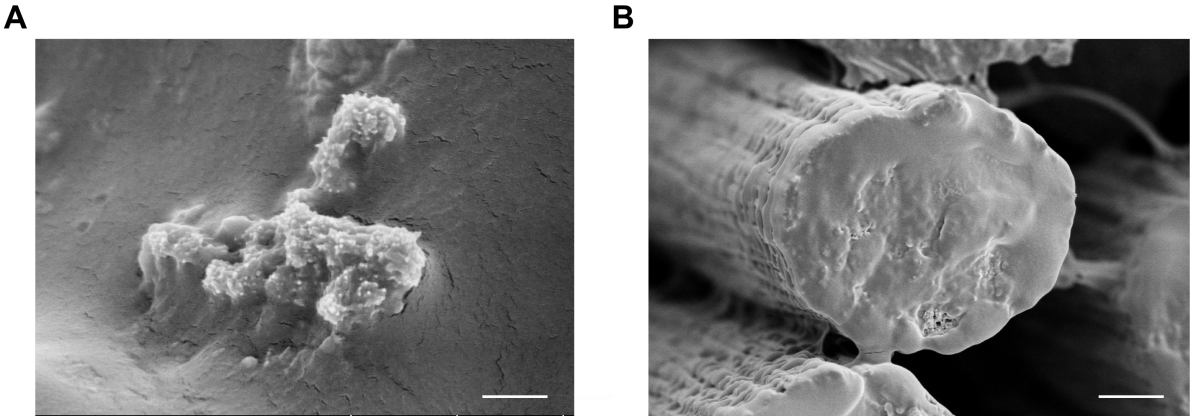

Figure S16. SEM image of nano-MnO_2 coated carbon fiber in (A) profile view and (B) cross section view. Taking measures of slurry coating method, nano-MnO_2 particles have been uniformly distributed around the fiber bundles, which ensures the stable electrochemical properties of ZIB fabrics. Scale bars, 5μm.

Tables

Table S1. Materials cost of GPHE-based ZIB.

Material	Price	Source
PVA	230.41 $/kg	Acros
$ZnSO_4$	26.75 $/kg	Innochem
$MnSO_4$	242.78 $/kg	Innochem
$K_2S_2O_8$	2474.28 $/kg	Innochem
GO Dispersion	1.55 $/kg	XFnano
Zn Foil	244.32 $/kg	Innochem
Silicone	9.90 $/kg	Alfa
PI Membrane	2.73 $/kg	Alfa
$Zn(CF_3SO_3)_2$	6976.74 $/kg	Innochem
$Zn(TFSI)_2$	127250.45 $/kg	Alfa

Table S2. Ion absorption of GPHE in salt solutions with different concentrations.

Samples	Mass concentration (mg/L) Zn:Mn		Molar concentration (mol/L) Zn:Mn		Average (mol/L)	
0.5 M $ZnSO_4$ 0.3 M $MnSO_4$	1.645	0.753	0.251	0.137	0.254	0.137
	1.671	0.747	0.257	0.136		
	1.668	0.756	0.256	0.138		
1.0 M $ZnSO_4$ 0.3 M $MnSO_4$	3.197	0.714	0.491	0.130	0.494	0.129
	3.202	0.712	0.492	0.129		
	3.233	0.703	0.500	0.128		
2.0 M $ZnSO_4$ 0.3 M $MnSO_4$	6.499	0.705	0.999	0.128	0.998	0.129
	6.457	0.715	0.993	0.130		
	6.534	0.708	1.004	0.129		

Table S3. A summary of electrolyte performances for zinc batteries.

Characterizations		Ref. 7	Ref. 21	Ref. 22	Ref. 23	Ref. 25	Ref. 31	Ref. 34	Ref. 35	This work
Mechanical Properties	Stretching Modulus (MPa)	-	0.120	34.5	-	-	1.67	557	-	1.03
	Elongation	-	920%	12.90%	-	200%	120%	4%	3000%	230%
Electrochemical Performance	Conductivity (mS/cm)	-	24.6	5.97	14.6	12.6	6.6	-	17.3	21.6
	Capacity (mAh/g)	125	148	167.6	260	77.2	96.7	21.7	102.6	172.5
	Efficiency after long cycle (%)	68.8%	90.42%	97.3%	49%	99.7%	95%	80%	98.5%	98%
	Current density/ Rate	0.5 C	6.5 C	1 A/g	1 C	1 A/g	1 A/g	1 A/g	2 A/g	2A/g
Self-healing Ability	Self-healing	-	-	Weak	-	Good	-	-	-	Good
Electrochemical Window	Electrochemical Window (V)	1.0 - 1.8	1.0 - 1.8	0.5 - 1.5	1.0 - 2.0	0.5 - 1.45	1.1 - 1.9	0.3 - 1.5	1.0 - 2.0	1.0 - 1.8
Price	Ingredients	low	medium	high	low	high	medium	high	high	low
Energy Storage System	Electrode	Zn-MnO_2	Zn-MnO_2	Zn-PANI	Zn-MnO_2	Zn-MnO_2	-	Zn-MnO_2	Zn-MnO_2	Zn-MnO_2
	Polymer	MWCNT/PET	ZSC-gel	PVA	Xanthan Gum	PVA	PAMPS-PAHz-PAAm	PCNF	PAM	GPHE
	Salt Solution	-	$ZnSO_4$ $MnSO_4$	$Zn(CF_3SO_3)_2$	$ZnSO_4$ $MnSO_4$	$Zn(CF_3SO_3)_2$	$ZnSO_4$	$Zn(CF_3SO_3)_2$	$ZnSO_4$ $MnSO_4$	$ZnSO_4$ $MnSO_4$

PAM, poly acrylamide; PVA, polyvinyl alcohol; PVAA, polyvinyl acetal; ZSC, zwitterionic sulfobetaine/cellulose; PDA, polydopamine; PAMPS-PAHz-PAAm, poly (2-Acrylamido-2-methyl-1-propanesulfonic acid) - polyacryloyl hydrazide - polyacrylamide; PCNF, polydopamine coated on carbon nanotube fibers.

Table S4. Elastic properties for FEA

Property	Value
E_{GPHE}	530 kPa
$E_{silicone}$	69 kPa
E_{Zn}	108 GPa
E_{Carbon}	235 GPa
v_{GPHE}	0.45
$v_{silicone}$	0.49
v_{Zn}	0.25
v_{Carbon}	0.27
ρ_{GPHE}	1.28 g/cm^3
$\rho_{silicone}$	1.28 g/cm^3
ρ_{Zn}	7.14 g/cm^3
ρ_{carbon}	1.77 g/cm^3

Movie S1.
Self-healing process of as-prepared GPHE after fracture

Movie S2.
Waterproof experiment in a standard washing machine

Movie S3.
Body state monitoring by the wireless chargeable TBAN and Blynk App